Appl Petrochem Res (2015) 5:363–369
DOI 10.1007/s13203-015-0111-4

ORIGINAL ARTICLE

Hydro-liquefaction of woody biomass for bio-oil in supercritical solvent with [BMIM]Cl/$NiCl_2$ catalyst

Qingyin Li[1,2] · Peng peng[1] · Dong Liu[1] · Min Li[1] · Linhua Song[2] · Mengfei Li[3] · Zifeng Yan[1] · Yiran Geng[4]

Received: 7 February 2015 / Accepted: 19 May 2015 / Published online: 4 June 2015

Abstract Thermochemical liquefaction characteristics of sawdust were explored with ethanol as solvent and [BMIM]Cl–$NiCl_2$ as catalyst. The influences of liquefaction parameters including reaction temperature, residence time and hydrogen initial pressure on the sawdust conversion and products distribution were studied. The maximum bio-oil yield of 75.45 % and conversion of 86.01 % were obtained in ethanol at 320 °C and 30 min under 10 MPa hydrogen pressure. The chemical composition of bio-oil and gaseous products derived from optimized conditions was analyzed via GC–MS and GC. These results showed that the dominant compounds of light oil were carboxylic acid, esters and phenol and its derivatives. In addition, the gaseous components consisted of CO_2, CO, methane, ethane and ethene.

Keywords Sawdust · Bio-oil · Hydro-liquefaction

✉ Dong Liu
ldongupc@vip.sina.com

✉ Zifeng Yan
zfyancat@upc.edu.cn

[1] State Key Laboratory of Heavy Oil Processing, PetroChina Key Laboratory of Catalysis, China University of Petroleum, Qingdao 266580, China

[2] College of Science, China University of Petroleum, Qingdao 266580, China

[3] College of Chemical Engineering, Qingdao University of Science and Technology, Qingdao 266580, China

[4] Hebei Baolong Occupation Hazard Detection Co.LTD, Shijiazhuang, 050093 China

Introduction

Excessive exploitation and environmental destruction have been fatalities for the utilization of coal, petroleum and gas currently. To deal with the depletion of fossil energy and environmental issues caused by the released carbon dioxide, biofuel was considered as one of the proposed solutions to substitute the usage of fossil fuel [1]. Generally, the biofuel generated from lignocellulose conversion had attracted more attentions [2]. The sawdust is an abundant residual forest biomass, which has not been utilized and is usually burned directly, leading to energy waste and environmental pollution. Thus, it is necessary to convert the residual to obtain bio-oil or useful chemicals through process techniques.

Thermochemical conversion processes including liquefaction, pyrolysis and gasification were employed to convert lignocellulose into liquid fuel [3–5]. Among these methods, liquefaction is a preferred technology due to its mild operation temperature, which could avoid cross linked and reverse reaction during liquefaction process. It is well known that the quality of bio-oil highly depended on the used solvent. The obtained bio-oil derived from biomass liquefaction with water as reaction medium has a lower carbon content and higher oxygen content, thus its heating value is much lower [6]. To enhance the heating value of liquid fuel, organic solvents were utilized in the lignocellulose conversion instead of water. Especially, the critical temperature and pressure of organic solvents are far below than that of water; therefore, the reaction could be carried out at milder conditions.

Among these organic solvents, from the viewpoint of environmental friendliness, ethanol could be the most promising solvent in the biomass conversion. On the other hand, it also has some advantages [7]. First, the critical points of ethanol are far below than that of water, so the

requirement for the operated equipment is lower. Second, as a hydrogen donor, ethanol can provide the active hydrogen to stabilize the produced intermediates. Third, the acidic components included in the bio-oil fractions can react with ethanol via esterification reaction to obtain ethyl esters compounds that are similar to biodiesel.

Recently, extensive researches have been received on the liquefaction of lignocellulose in the ethanol. Huang et al. [8] investigated the liquefaction of rice husk with ethanol as solvent, and effect of different reaction parameters on the liquefaction behavior was also discussed. Liu and his co-workers reported the reaction pathways of cornstalk liquefaction in sub- and supercritical ethanol [9].

Ionic liquids have attracted increasing attention for dissolution of biomass and its components, which can destroy the hydrogen bond in the covalent structure for the further utilization of sustainable feedstock [10, 11]. Many researchers have reported that the ionic liquid was adopted for the dissolution of material including microcrystalline and woody biomass [12, 13]. In the study, $NiCl_2$ was utilized as hydrogenation catalyst in the direct liquefaction of biomass. Besides, the introduced ionic liquid [BMIM]Cl in the reaction system can form the corresponding ionic liquid nickel catalyst, which may improve the catalytic activity and thus enhance the biofuel yield. The metal ions in ionic liquid catalyst also have been investigated in the microcrystalline conversion [14].

To the best of the authors' knowledge, no previous study describing the thermochemical liquefaction characteristics of sawdust in supercritical ethanol with [BMIM]Cl–$NiCl_2$ as catalyst has been reported. In this work, liquefaction of sawdust in ethanol with [BMIM]Cl–$NiCl_2$ was investigated. The influence of reaction temperature, time and hydrogen initial pressure on the liquefaction of sawdust was studied. Furthermore, the obtained bio-oil and gaseous product were characterized using gas chromatography–mass spectrometry (GC–MS) and gas chromatography (GC), respectively. The solid residue was characterized by X-ray diffraction (XRD).

Experimental

Materials

The sawdust used in this study was obtained from wood industry, and was ground with a high-speed rotary cutting mill and sieved to 60 mesh. The elemental and chemical compositions of raw material are given in Table 1. The ionic liquid [BMIM]Cl was synthesized according to the previous literature [15]. The utilized analytical research grade solvents (acetone and ethanol) and $NiCl_2$ were purchased from Sinopharm Chemical Reagent Co., Ltd. The high-pressure micro-autoclave was made in the lab.

Table 1 Chemical and elemental compositions of sawdust

Elemental composition (wt%)		Chemical composition (wt%)	
C	47.68	cellulose	48.27
H	6.30	hemicellulose	19.50
N	0.45	lignin	19.80
O[a]	45.57	extractives	11.40
		ash	0.97
HHV/MJ kg^{-1}	17.00		

The chemical components including cellulose, hemicellulose, lignin, extractives and ash were determined via Van Soest method [16]. The elemental analysis (C, H and N) was carried out with an elemental analyzer (Vario EL III). The content of oxygen was estimated by difference. The Higher Heating Value (HHV) was calculated based on the Dulong formula [17, 18].

$$\begin{aligned} \mathrm{HHV(MJ/kg)} &= 338.2\ \mathrm{wt\%}\ \ (\mathrm{C}) \\ &\quad + 1442.8\ (\mathrm{wt\%}\ (\mathrm{H}) - \mathrm{wt\%(O)}/8). \end{aligned} \tag{1}$$

Experimental procedures and products separation

In each experiment, 1 g of sawdust, 10 ml of ethanol, 1.2 wt% [BMIM]Cl and 300 μg/g Ni-based catalyst were charged into the reactor. Subsequently, the reactor was sealed, and the inside air was displaced by hydrogen with three times and then the pressure was elevated to the desired pressure. The reactor was heated up to the desired temperature in a molten-tin bath. After the experimentally desired time, the reactor was immersed into a cooled water bath to terminate the reaction. The procedure for separation of gas, liquid and solid products is shown in Fig. 1.

After each run, the gas was collected for components analysis. The liquid–solid suspension products were thoroughly rinsed from the reactor with ethanol, and then were filtered using a pre-weighed filter paper. The obtained solid residue was extracted with ethanol and acetone until the eluate was colorless, respectively. The solid product remaining on the paper was dried at 105 °C and weighed. The dried residue was defined as the solid residue (SR). The ethanol and acetone solutions were evaporated to remove solvents, and the resulted liquids were denoted as light oil (LO) and heavy oil (HO).

The yields and conversion of products are defined as follows:

$$\text{Yield of light oil} = \frac{\text{mass of light oil}}{\text{mass of sawdust}} \times 100\,\% \tag{2}$$

$$\text{Yield of heavy oil} = \frac{\text{mass of heavy oil}}{\text{mass of sawdust}} \times 100\,\% \tag{3}$$

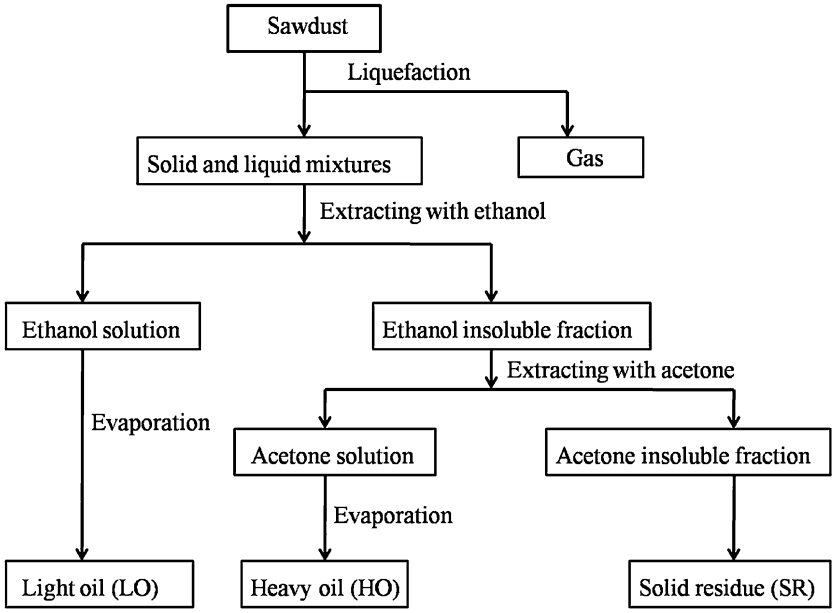

Fig. 1 Products separation and analysis

$$\text{Yield of residue} = \frac{\text{mass of residue}}{\text{mass of sawdust}} \times 100\,\% \quad (4)$$

$$\text{Yield of gas} = 100\%\text{-yield of bio-oil-yield of residue.} \quad (5)$$

Characterization

The collected gaseous products were analyzed and quantified using a gas chromatography (CP-3800) with a 5 m Porapak Q column and a TCD detector. The specified chemical compositions of bio-oil were analyzed by gas chromatography–mass spectrometry (GC–MS, Thermo Fisher Scientific, Trace). An Agilent model DB-35MS column (30 m × 0.25 mm × 0.25 μm) was equipped on a Trace GC–MS system. The identification of compounds was based on the computer matching of mass spectra from National Institute of Standard and Technology (NIST) library. The details on the GC–MS operation were given in our previous paper [19]. The X-ray diffraction (XRD) measurements for solid residue were carried out using Cu Kα radiation ($\lambda = 1.5406$ Å) with a Rigaku D/MAX-IIIC X-ray diffractometer.

Results and discussion

Effect of temperature

Figure 2 illustrates the influence of reaction temperature on the product yields at 40 min and 4.0 MPa hydrogen initial pressure by varying temperature from 300 to 350 °C.

Over the whole range of tested temperatures, the solid residue yield declined rapidly from 44.00 to 19.57 %. On the contrary, the gaseous yield showed a different trend with increasing temperature. The highest gas yield of 41.97 % could be observed at 350 °C. First, the increasing bio-oil yield was found to be more evident as the temperature climbed from 300 to 320 °C. However, the further increase in temperature could lead to decrease in the bio-oil yield, which suggested thermal cracking of bio-oil at the temperature higher than 320 °C.

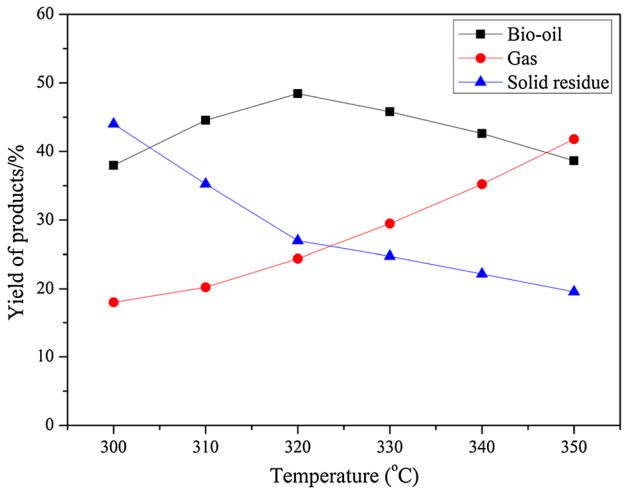

Fig. 2 Effect of temperature on the yield of products

Biomass was broken down to some fragments and then these fragments were decomposed to smaller compounds, and the produced compounds could be rearranged through condensation, cyclization and polymerization to form new ones [20]. Clearly, the higher temperature facilitated the formation of gas and bio-oil. As the temperature exceeded 320 °C, the produced compounds could break down into

comparatively smaller and more volatile fractions. Beyond the critical temperature, the decomposition of bio-oil into gaseous products was the dominant reaction in the liquefaction process, which was consistent with the result of increasing gas yield. In summary, the higher temperature would result in the occurrence of cracking, gasification and fragment of liquid and solid products.

Effect of hydrogen initial pressure

The effect of hydrogen initial pressures from 2 to 10 MPa on the liquefaction characteristics of sawdust is depicted in Fig. 3. The operation hydrogen initial pressure significantly affects the product distributions. For the whole hydrogen pressure, the bio-oil yield was increased monotonically with increasing pressure, and the bio-oil yield appeared to be maximized under 10 MPa hydrogen pressure.

Generally, hydrogen gas plays an important role in the formation of bio-oil. During the liquefaction process, the intermediates produced may be stabilized immediately by the hydrogen free radicals to form the liquid products. The higher the hydrogen initial pressure, the more the hydrogen free radicals produced. The free radicals from the decomposition of sawdust could be stabilized well under the higher hydrogen pressure, which prevented the condensation, cyclization and re-polymerization reactions [21]. On the other hand, the higher the system pressure obtained, the lesser the liquid components would be gasified.

The above-mentioned viewpoint may also explain the fact that the solid residue formation was reduced, which was ascribed to that condensation of liquid product was restrained. The increase in the pressure inside the reactor is unfavorable to the formation of gaseous products. Thus, the gas yield decreased slightly with increasing hydrogen initial pressure.

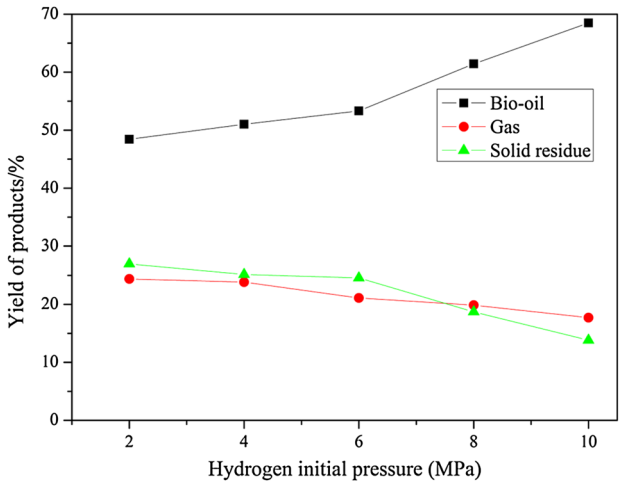

Fig. 3 Effect of hydrogen initial pressure on the yield of products

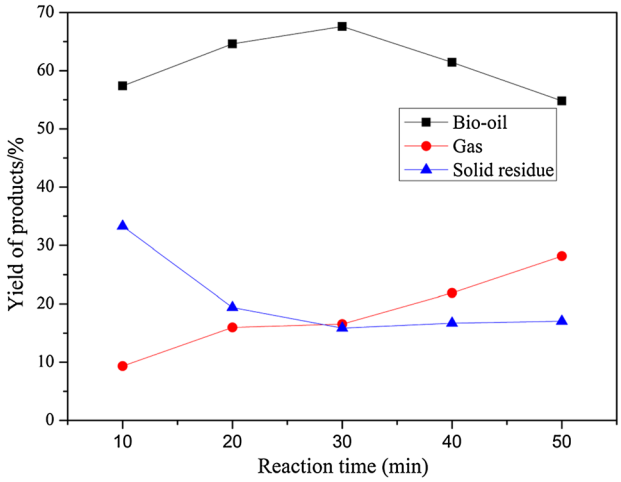

Fig. 4 Effect of time on the yield of products

Effect of time

Figure 4 illustrates the yield of different products from hydro-liquefaction of sawdust at 320 °C under 8 MPa with varying holding time, from 10 to 50 min.

The bio-oil yield increased from 57.39 to 67.6 % as the reaction time increased from 10 to 30 min. However, the prolonged time could result in a significant decrease in the liquid yield due to further degradation of the bio-oil, and the highest bio-oil yield could be achieved at 30 min. As shown in Fig. 3, the gaseous yield increased gradually in the whole residence time. It could be explained that decomposition of large bio-oil molecule occurred at a longer time. The produced large fragments would be converted to smaller and more volatile ones, leading to the bio-oil yield decline.

It was noted that the yield of solid residue decreased with increasing time from 10 to 30 min. Further increase in time would enhance the formation of solid residue due to the condensation and re-polymerization of intermediates, which could lower the bio-oil yield accordingly.

Products characterization

GC–MS

The GC–MS analysis of light oil and heavy oil derived from the optimal conditions (320 °C, 30 min and 10 MPa hydrogen initial pressure) showed that liquefaction of sawdust is a more complex process. The compounds listed in Tables 2 and 3 are those represented by peak areas larger than 1 % of total.

Furthermore, to better understand the component distributions in different oil fractions, the compounds in bio-oils are categorized into different groups according to functional groups, as shown in Fig. 5.

Table 2 The main compounds in the ethanol soluble oil determined by GC–MS

No	Residence time/min	Molecular formula	Compound types	Relative content (%)
1	4.7	CH_3COOH	Formic acid	3.06
2	5.56	$C_4H_8O_3$	Ethyl 2-hydroxyacetate	5.15
3	5.82	$C_5H_{10}O_3$	Ethyl 2-hydroxypropanoate	4.54
4	7.1	$C_6H_{12}O_3$	Ethyl 2-hydroxybutanoate	1.98
5	7.2	$C_5H_{10}O_2$	2-ethyl-1,3-dioxolane	2.72
6	9.16	C_6H_6O	Phenol	1.03
7	9.38	$C_7H_{16}O$	Heptan-4-ol	1.87
8	11.34	$C_7H_{12}O_3$	Ethyl 4-oxopentanoate	1.53
9	11.8	$C_6H_{12}O_2$	Ethyl isobutyrate	7.45
10	12.39	$C_7H_8O_2$	2-methoxyphenol	1.52
11	13.58	$C_8H_{12}O_2$	2-ethyl-2-methylcyclopentane-1,3-dione	1.21
12	14	$C_8H_{14}O_4$	Diethyl succinate	4.51
13	14.51	$C_9H_{16}O_4$	Diethyl 2-methylsuccinate	1.52
14	14.97	$C_9H_{20}O$	4-methyloctan-4-ol	1.29
15	15.73	$C_9H_{16}O_4$	Diethyl glutarate	1.89
16	15.9	$C_9H_{12}O_2$	4-ethyl-2-methoxyphenol	3.28
17	16.31	$C_{10}H_{20}O_2$	Methyl 2-isopropyl-3,3-dimethylbutanoate	1.83
18	17.01	$C_{10}H_{14}O_2$	2-methoxy-4-propylphenol	7.43
19	17.94	$C_{10}H_{12}O_2$	(E)-2-methoxy-4-(prop-1-en-1-yl) phenol	4.07
20	18.51	$C_{10}H_{14}O_3$	5-isopropylbenzene-1,2,3-triol	2.37
21	19.1	$C_9H_8O_5$	5-(1-hydroxyvinyl)-2-methoxybenzoic acid	5.33
22	19.58	$C_{16}H_{18}$	(Z)-1,2,3-trimethyl-4-(prop-1-en-1-yl)naphthalene	5.21
23	19.75	$C_{11}H_{14}O_3$	(Z)-2,6-dimethoxy-4-(prop-1-en-1-yl)phenol	5.33
24	23.00	$C_{17}H_{34}O_2$	Heptadecanoic acid	1.46

Table 3 The main compounds in the acetone soluble oil determined by GC–MS

No	Residence time/min	Molecular formula	Compound types	Relative content (%)
1	12.15	$C_8H_{14}O_3$	Isobutyric anhydride	7.55
2	12.38	$C_{10}H_{14}O$	2-phenylbutan-2-ol	1.5
3	13.56	$C_{11}H_{12}O_2$	Phenyl 3-methylbut-2-enoate	2.58
4	14.6	$C_{10}H_{22}O_2$	3,7-dimethyloctane-1,7-diol	3.06
5	16.66	$C_6H_{14}O_5$	3,3′-dimethyloctane-1,7-diol	34.06
6	18.11	$C_9H_{10}O_2$	1-(4-hydroxy-2-methylphenyl)ethanone	2.08
7	18.36	$C_9H_{12}O_3$	1,2,4-trimethoxybenzene	2.82
8	18.6	$C_9H_{12}O_3$	1,2,3-trimethoxybenzene	3.1
9	18.98	$C_9H_8O_5$	4-methoxyisophthalic acid	2.31
10	19.38	$C_{12}H_{20}O_2$	(2-ethoxy-2,3,3a,4,7,7a-hexahydro-1H-inden-1-yl)methanol	7.35
11	20.1	$C_{18}H_{22}N_2O$	3,3-dimethyl-1-methylene-N-propyl-1,2,3,4-tetrahydroacridin-9-amine	1.06
12	21.14	$C_{19}H_{38}O_2$	Ethyl palmitate	1.93
13	22.5	$C_{18}H_{32}O_3$	3-tetradecyl dihydrofuran-2,5-dione	1.02
14	23.01	$C_{20}H_{18}O_6$	8-ethyl-1,6,8,11-tetrahydroxy-7,8,9,10-tetrahydrotetracene-5,12-dione	1.61
15	23.27	$C_{21}H_{42}O_2$	Ethyl stearate	2.34
16	23.52	$C_{20}H_{42}O_2$	1-ethoxyoctadecane	3.56
17	24.04	$C_{22}H_{44}O_2$	Ethyl nonadecanoate	4.87
18	25.24	$C_{24}H_{48}O_2$	Ethyl henicosanoate	2.84
19	26.77	$C_{25}H_{50}O_2$	Methyl 2,3-dimethylicosanoate	3.96
20	27.88	$C_{26}H_{52}O_2$	Methyl henicosanoate	1.06
21	29.28	$C_{28}H_{56}O_2$	Methyl 2,10-dimethylhenicosanoate	1.06

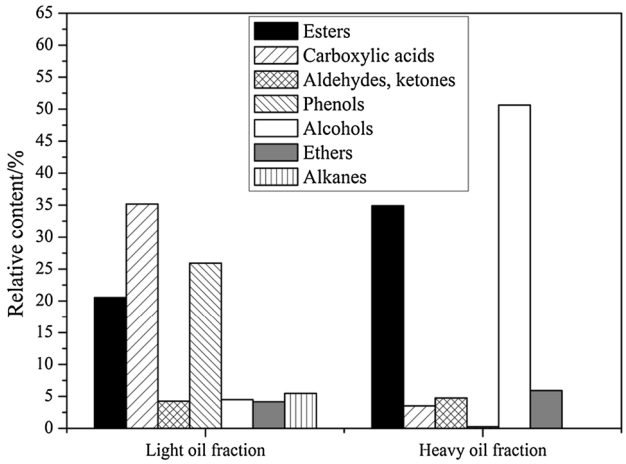

Fig. 5 Compositions of light oil and heavy oil categorized by oxygenated functional groups

The compounds are categorized against their functional groups to form seven groups: esters, carboxylic acids, aldehydes and ketones, phenols, alcohols, ethers and alkanes. The light oil fraction mainly contained esters, carboxylic acids and phenols compounds, whereas alcohols and esters are majority in the heavy oil fraction. It should be noted that some non-volatile compounds with large molecular weight could not pass through the gas chromatographic column; therefore, some products such as phenolic derivatives in the heavy oil fraction were unable to be detected.

The formation of esters was mainly attributed to the reaction between ethanol and carboxylic acid. As reported in the previous literatures, the carboxylic acid could be formed via complex alcoholysis and dehydration of cellulose and hemicellulose components, and then the produced acids could react with ethanol by esterification reaction to obtain fatty acid esters [22].

On the other hand, the phenolic compounds and derivatives are originated from decomposition of lignin component in the biomass through the cleavage of the aryl ether linkages [23]. Additionally, the condensation and cyclization of carbohydrate intermediates would also lead to the formation of phenolic compounds [24, 25].

GC analysis

The GC analysis of gaseous products from sawdust conversion under the optimal condition is shown in Fig. 6.

The gaseous compositions consisted of methane, ethane, ethene, carbon dioxide and carbon monoxide. The relative mass percentage of carbon dioxide and carbon monoxide was lower than that of hydrocarbons. The formation of CO_2 and CO is produced through degradation of oxygen-containing groups in the intermediate and products via decarbonylation and decarboxylation [26].

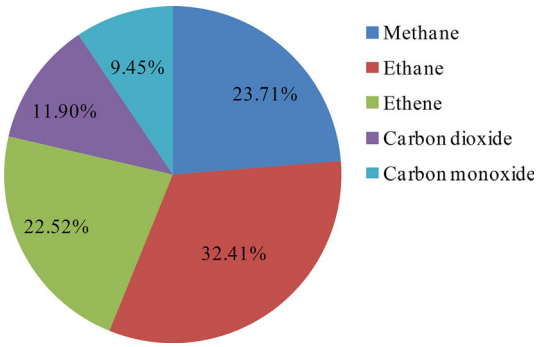

Fig. 6 The gaseous component from sawdust liquefaction at 320 °C and 30 min under 10 MPa hydrogen initial pressure

Besides, methane could be formed by the decomposition of methoxyl groups in the unit of lignin. It should be noted that ethane was found to be the dominant fraction in the gas. The similar result was observed by Brand et al. in the liquefaction of lignocellulose with ethanol as the medium [27]. The ethane and ethene products were mainly generated from the supercritical ethanol decomposition, which suggested that ethanol could provide active hydrogen to stabilize the produced fragments during the sawdust liquefaction.

XRD characterization

Figure 7 shows the XRD patterns of sawdust and solid residue obtained under the optimal conditions. Three characteristic peaks at $2\theta = 14.7°$, 16.5° and 22.4° from the diffraction on the 110, $1\bar{1}0$ and 002 planes of cellulose I were clearly observable in the raw material [28]. On the contrary, the characteristic peaks derived from cellulose I disappeared in the solid residue, which suggested that the cellulose crystalline structure in the sawdust was completely degraded. Additionally, this result also indicated

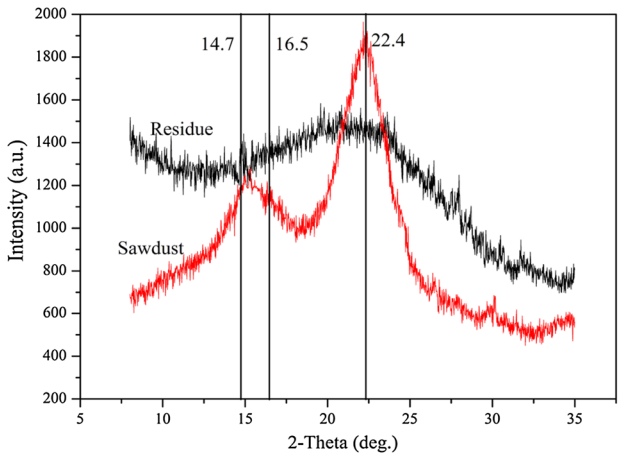

Fig. 7 XRD patterns of sawdust before and after liquefaction at 320 °C and 30 min under 10 MPa hydrogen pressure

that the liquefaction reaction of sawdust took place in the experimental conditions.

Conclusion

In this work, sawdust was effectively liquefied in supercritical ethanol with [BMIM]Cl–$NiCl_2$ as catalyst. The maximum bio-oil yield was 75.45 % with optimal conversion of 86.01 % at 320 °C and 30 min under 10 MPa hydrogen initial pressure. According to the GC–MS results, the majorities in the light oil fraction were carboxylic acids, esters and phenolic compounds. By contrast, the main components in heavy oil fraction were esters and alcohols. The GC results revealed that the gaseous products mainly included methane, ethane and ethene. Besides, the XRD result showed that the crystalline structure in the sawdust was destroyed after liquefaction reaction.

Acknowledgments This work was financially supported by National Nature Science Foundation of China (21176259), Funds of Development of Science and Technology of China National Petroleum Corporation (No. 2013A-2106), the Joint Funds of the National Natural Science Foundation of China and China National Petroleum Corporation (Grant No. U1362202).

References

1. Gan J, Yuan W-Q (2013) Operating condition optimization of corncob hydrothermal conversion for bio-oil production. Appl Energy 103:350–357
2. Baratieri M, Baggio P, Fiori L, Grigiante M (2008) Biomass as an energy source: thermodynamic constraints on the performance of the conversion process. Bioresour Technol 99:7063–7073
3. Heo H-S, Park H-J, Dong J-I, Park H-S, Kim S, Suh D-J, Suh Y-W, Kim S-S, Park Y-K (2010) Fast pyrolysis of rice husk under different reaction conditions. J. Ind. and Eng. Chem. 16:27–31
4. Madhiyanon T, Sathitruangsak P, Soponronnarit S (2011) Influence of coal size and coal-feeding location in co-firing with rice husks on performance of a short-combustion-chamber fluidized-bed combustor (SFBC). Fuel Process Technol 92:462–470
5. Loha C, Chattopadhyay H, Chatterjee P-K (2011) Thermodynamic analysis of hydrogen rich synthetic gas generation from fluidized bed gasification of rice husk. Energy 36:4063–4071
6. Matsumura Y, Nonaka H, Yokura H, Tsutsumi A, Yoshida K (1999) Co-liquefaction of coal and cellulose in supercritical water. Energy Fuels 78:1049–1056
7. Jade C, Pattarapan P (2010) Bio-oil from hydro-liquefaction of bagasse in supercritical ethanol. Energy Fuels 24:2071–2077
8. Huang H-J, Yuan X-Z, Zeng G-M, Liu Y, Li H, Yin J, Wang X-L (2013) Thermochemical liquefaction of rice husk for bio-oil production with sub- and supercritical ethanol as solvent. J Anal Appl Pyrolysis 102:60–67
9. Liu H-M, Xie X-A, Ren J-L, Sun R-C (2012) 8-Lump reaction pathways of cornstalk liquefacton in sub- and super-critical ethanol. Ind Crops Prod 35:250–256
10. Fort D-A, Remsing R-C, Swatloski R-P, Moyna G, Rogers R-D (2007) Can ionic liquids dissolve wood ? Processing and analysis of lignocellulosic materials with 1-*n*-butyl-3-methylimidazolium chloride. Green Chem 9:63–69
11. Kilpelainen I, Xie H-B, King A, Granstrom M, Heikkinen S, Argyropoulos DS (2007) Dissolution of wood in ionic liquids. J Agric Food Chem 22:9142–9148
12. Swatloski R-P, Spear S-K, Holbrey J-D, Roger R-D (2002) Dissolution of cellulose with ionic liquids. J Am Chem Soc 124:4974–4975
13. Lee S-H, Doherty T-V, Linhardt R-J, Dordick J-S (2009) Ionic liquid -mediated selective extraction of lignin from wood leading to enhanced enzymatic cellulose hydrolysis. Biothchnol. Bioeng. 102:1368–1376
14. Tao F-R, Song H-L, Chou L-J (2012) Efficient conversion of cellulose into furans catalyzed by metal ions in ionic liquids. J Mol Catal A: Chem 357:11–18
15. Burrell A-K, Del Sesto R-E, Baker S-N, McCleskey T-M, Baker G-A (2007) The large scale synthesis of pure imidazolium and pyrrolidinium ionic liquids. Green Chem 9:449–454
16. Van Soest P-J, Wine R-H (1967) Use of detergents in the analysis of fibrous feed. IV. Determination of plant cell-wall constituents. J. Assoc. Off. Agric. Chem. 50:50–55
17. Zhong C, Wei X (2004) A comparative experimental study on the liquefaction of wood. Energy 29:1731–1741
18. Huang H-J, Yuan X-Z, Zeng G-M, Wang J-Y, Li H, Zhou C-F, Pei X-K, You Q, Chen L (2011) Thermochemical liquefaction characteristics of microalgae in sub- and supercritical ethanol. Fuel Process Technol 92:147–153
19. Li Q-Y, Liu D, Song L-H, Wu P-P, Yan Z-F (2014) Direct liquefaction of sawdust in supercritical alcohol over ionic liquid nickel catalyst: effect of solvents. Energy Fuels 28:6928–6935
20. Wang G, Li W, Li B-Q, Chen H-K (2007) Direct liquefaction of sawdust under syngas. Fuel 86:1587–1593
21. Kucuk M-M, Agirtas S (1999) Liquefaction of *Prangmites australis* by supercritical gas extraction. Bioresour Technol 69:141–143
22. Peterson A-A, Vogel F, Lachance R-P, Fröling M, Antal M-J, Tester J-W (2008) Thermochemical biofuel production in hydrothermal media: a review of sub- and supercritical water technologies. Energy Environ Sci 1:32–65
23. Sun P-Q, Heng M-X, Sun S-H, Chen J-W (2011) Analysis of liquid and solid products from liquefaction of paulownia in hot-compressed water. Energy Convers Manage 52:924–933
24. Nelson D-A, Landsman S-D, Molton P-M (1984) Formation, during liquefaction of cellulose, of 2,5-dimethyl-1, 4-benzenediol via aldol addition and a reduction–oxidation. Carbohyd Res 128:356–360
25. Sinag A, Kruse A, Schwarzkopf V (2003) Key compounds of the hydropyrolysis of glucose in supercritical water in the presence of K_2CO_3. Ind Eng Res. 42:3519–3521
26. Marx S, Chiyanzu I, Piyo N (2014) Influence of reaction atmosphere and solvent on biochar yield and characteristics. Bioresour Technol 164:177–183
27. Brand S, Susanti R-F, Kim S-K, Lee H-S, Kim J, Sang B-I (2013) Supercritical ethanol as an enhanced medium for lignocellulosic biomass liquefaction: Influence of physical process parameters. Energy 59:173–182
28. Zhang J, Kamdem D-P (2000) X-ray diffraction as an analytical method in wood preservatives. Holzforschung 54:27–32